EPR Investigation of Persistent Radicals Produced from the Photolysis of Dibenzyl Ketones Adsorbed on ZSM-5 Zeolites

Nicholas J. Turro,*,† Xue-gong Lei,† Steffen Jockusch,† Wei Li,† Zhiqiang Liu,† Lloyd Abrams,§ and M. Francesca Ottaviani‡

Department of Chemistry, Columbia University, New York, New York 10027, Institute of Chemical Sciences, University of Urbino, Piazza Rinascimento, 6 Urbino, Italy 61029, and E. I. Dupont, Central Research, Experimental Station, Wilmington, Delaware 19880

turro@chem.columbia.edu

Received November 5, 2001

Photolysis of ketones (**1**, **1**-oMe, **2**, **2**-oMe, **3**, and **4**) adsorbed on ZSM-5 zeolites produces persistent carbon-centered radicals that can be readily observed by conventional steady-state EPR spectroscopy. The radicals are persistent for time periods of seconds to many hours depending on the supramolecular structure of the initial radical@zeolite complex and the diffusion and reaction dynamics of radicals produced by photolysis. The structures of the persistent radicals responsible for the observed EPR spectra are determined by a combination of alternate methods of generation of the same radical, by deuterium substitution, and by spectral simulation. A clear requirement for persistence is that the radicals produced by photolysis must either separate and diffuse from the external to the internal surface or be generated within the internal surface and separate and diffuse apart. The persistence of radicals located on the internal surface is the result of inhibition of radical−radical reactions. Radicals that are produced on the external surface and whose molecular structure prevents diffusion into the internal surface are transient because radical−radical reactions occur rapidly on the external surface. The reactions of the persistent radicals with oxygen and nitric oxide were directly studied in situ by EPR analysis. In the case of reaction with oxygen, persistent peroxy radicals are formed in high yield. The addition of nitric oxide scavenges persistent radicals and leads initially to a diamagnetic nitroso compound, which is transformed into a persistent nitroxide radical by further photolysis. The influence of variation of radical structure on transience/persistence is discussed and correlated with supramolecular structure and reactivity of the radicals and their parent ketones.

Introduction

In organic chemistry, carbon-centered free radicals are generally considered to be transient reactive intermediates, as the result of the inherent fast rates of reactions of radicals with molecules and of reactions of radicals with other radicals.[1] Even if "inert " solvents are employed to remove radical−molecule reactions, radical−radical reactions (combination and disproportionation) that typically occur at or near the diffusion rate for simple carbon-centered radicals will limit the radical lifetime to the microsecond to millisecond domain.[2] The term "persistence" has been suggested[3] to describe a radical that has a significant lifetime compared to some standard, "transient" radical, under similar conditions in nonviscous solvents. In this report, we operationally define radicals that are produced in zeolites and that are readily detected by conventional steady-state CW EPR at room temperature as "persistent" and radicals that are produced but cannot be detected by steady-state EPR as "transient". This operational definition implies that the radicals that possess "lifetimes" on the order of seconds or longer will be persistent and detectable by CW EPR. This is a very long time scale compared to the lifetimes (e.g., microseconds to milliseconds) of carbon-centered radicals in nonviscous fluid solutions.[2]

Carbon-centered radicals in inert solvents can be rendered persistent through intramolecular steric factors that slow radical−radical reactions.[3] For example, in the case of the classic triphenyl methyl radical,[4] the three phenyl groups form a twisted propeller environment which sterically inhibits radical−radical reaction at the trivalent carbon atom. Similar steric effects are responsible for the persistence[3,5] of other carbon-centered radicals in solution. The idea of molecular steric stabilization of radicals has been adapted to design *supramolecular* steric stabilization to render radicals persistent.[6] These studies have shown that benzyl and related carbon-centered radicals, which are transient and undergo radical−radical reactions at close to the diffusion-controlled rate in fluid solutions,[2] can be rendered persistent when they are created by the photolysis of ketones adsorbed on zeolites.[6,7] However, not all benzyl

† Columbia University.
‡ University of Urbino.
§ E. I. Dupont. Contribution No. 8198.

(1) Fischer, H.; Radom, L. *Angew. Chem.* **2001**, *40*, 1340−1371, and references therein.
(2) Schuh, H.-H.; Fischer, H. *Helv. Chim. Acta* **1978**, *61*, 2130−2164.
(3) Griller, D.; Ingold, K. U. *Acc. Chem. Res.* **1976**, 9, 13−19.
(4) (a) Gomberg, M. *Ber.* **1900**, *33*, 3150−3163; *J. Am. Chem. Soc.* **1900**, *22*, 757−771. (b) McBride, J. M. *Tetrahedron* **1974**, *30*, 2009−2022.
(5) Lankamp, H.; Nauta, W. T.; MacLean, C. *Tetrahedron Lett.* **1968**, 249−254.
(6) (a) Hirano, T.; Li, W.; Abrams, L.; Krusic, P. J.; Ottaviani, M. F.; Turro, N. J. *J. Am. Chem. Soc.* **1999**, *121*, 7170−7171. (b) Turro, N. J. *Acc. Chem. Res.* **2000**, *33*, 637−646.

10.1021/jo011047l CCC: $22.00
Published on Web 00/00/0000 PAGE EST: 12.9

Chart 1. Structures of Ketones Investigated in This Report

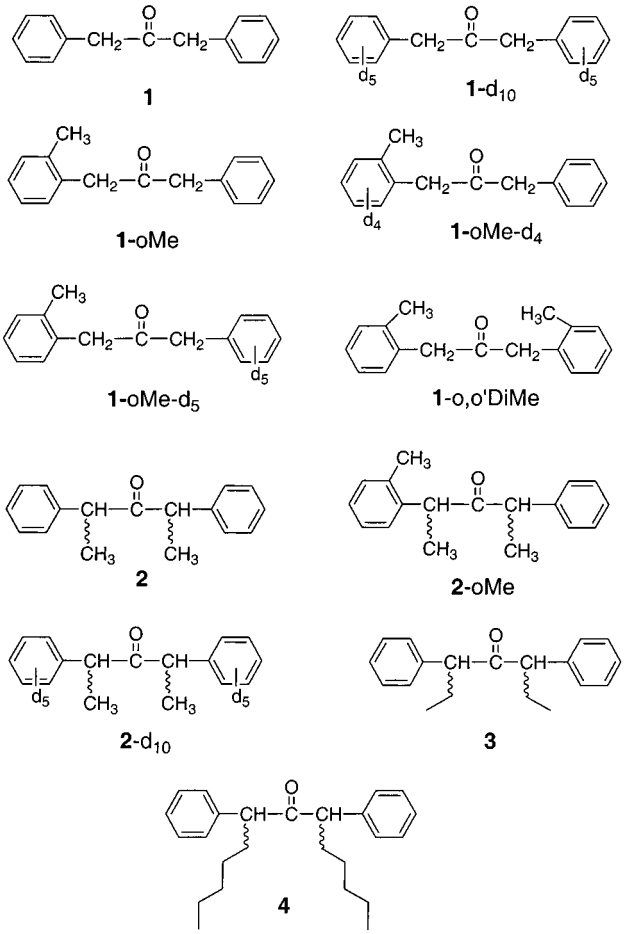

type radicals produced in this manner are persistent. The proposed mechanism of radical persistence has been attributed to supramolecular steric effects and to dynamic diffusional and/or structural constraints imposed by the adsorption of radicals on the internal surface of zeolites which inhibit radical−radical reactions.[6]

We report here an EPR investigation of the influence of supramolecular structure and dynamics on the persistence of a family of carbon-centered radicals produced by photolysis of "guest" ketones **1**, **1**-oMe, **2**, **2**-oMe, **3**, and **4** (Chart 1) adsorbed on a "host" ZSM-5 zeolite. We shall demonstrate that persistence and transience of radicals adsorbed on zeolites can be predicted from knowledge of the initial supramolecular structure and dynamics of the guest@host complexes (the @ represents noncovalent binding of the guest and host) that are photolyzed. The results demonstrate that, to be persistent, the radicals produced by photolysis must either separate and diffuse from the external to the internal surface or be generated within the internal surface and separate and diffuse apart. Radicals that are produced on the external surface and whose molecular structure prevents diffusion into the internal surface are transient; that is, they react too rapidly to be detected by steady-state EPR analysis.

Supramolecular Photochemistry of Organic Molecules Adsorbed on Zeolites. In molecular organic chemistry, covalent bonds are critical in determining molecular chemical structure and reactivity, whereas in supramolecular organic chemistry noncovalent bonds are critical in determining supramolecular structure and reactivity. The "guest@host" paradigm[8−10] inspired by the chemistry of enzymes provides a useful working model for supramolecular chemistry. In this paradigm the concept of the *molecular* "solvent cage" is translated to the *supramolecular* "supercage" which holds together guest molecules (or reactive intermediates) by providing a cage with "walls" of varying degrees of hardness or softness through noncovalent bonds.

In this report the guests are a series of dibenzyl ketones (Chart 1), and the host is ZSM-5 crystals, members of the MFI family of zeolites.[11] The host was selected because of its importance in the catalytic sciences, which results from the size/shape selectivity of ZSM-5 zeolites for adsorption of guests whose dimensions are of the size of a benzene ring.[12] MFI crystals possessing Si/Al < 80 are termed MZSM-5, where M represents an exchangeable cation. In this report, Si/Al = 20, M = Na, and the term ZSM-5 will be used to describe the zeolite crystals. The adsorption of ketones onto a MFI crystal produces supramolecular ketone@MFI complexes on the external or internal surface, depending on the size/shape relationships of the guest and the host void space.

In addition to the structural variations of the guest and host just described, the variation of the loading (weight of ketone adsorbed on a given weight of zeolite) provides a means of varying the supramolecular structure of the ketone@ZSM-5 complexes also. The reason for this is that there are several different host binding sites which are fixed in number depending on the surface area (external or internal) of the zeolite, and as the loading of ketone is varied, the occupancy or coverage of the binding sites will change. Although the molecular structures of the host and guest are not significantly changed by variation of coverage of the host surface, we shall show that the supramolecular structure and dynamics, and as a consequence, the supramolecular reactivity of ketone@ZSM-5, may change dramatically with coverage.

Size/shape characteristics are important factors in determining molecular adsorption capacity and diffusion

(7) (a) Turro, N. J.; Lei, X.; Li, W.; McDermott, A.; Abrams, L.; Ottaviani, M. F.; Beard, H. S. *Chem. Commun.* **1998**, 695−696. (b) Turro, N. J.; McDermott, A.; Lei, X.; Li, W.; Abrams, L.; Ottaviani, M. F.; Beard, H. S.; Houk, K. N.; Beno, B. R.; Lee, P. S. *Chem. Commun.* **1998**, 697−698.

(8) Lehn, J. M. *Supramolecular Chemistry*; VCH: New York, 1995.

(9) Herron, N. *Chemtech* **1989**, 542−548.

(10) Parton, R.; De Vos, D.; Jacobs, P. A. Enzyme Mimicking with Zeolites. In *Zeolite Microporous Solids: Synthesis, Structure and Reactivity*; Derouane, E. G., Lemos, F., Naccache, E., Ribeiro, F. R., Eds.; Kluwer Academic Publishers: Dordrecht, 1992; pp 555−578.

(11) (a) Meier, W. M.; Olson, D. H. *Atlas of Zeolite Structure Types*; Butterworth-Heinemann: London, 1992. (b) Breck, D. W. *Zeolite Molecular Sieves: Structure, Chemistry, and Use*; Wiley and Sons: London, 1974. (c) Szostak, R. *Molecular Sieves: Principle of Synthesis and Identification*; Van Nostrand Reinhold: New York, 1989. (d) Flanigen, E. M.; Bennet, J. M.; Grose, R. W.; Cohen, J. P.; Patton, R. L.; Kirchner, R. M.; Smith, J. V. *Nature* (*London*) **1978**, *272*, 512−516. (e) Kokotailo, G. T.; Lawton, S. L.; Olson, D. H.; Meier, W. M. *Nature* (*London*) **1978**, *272*, 437−438. (f) Olson, D. H.; Kokotailo, G. T.; Lawton, S. L.; Meier, W. M. *J. Phys. Chem.* **1981**, *85*, 2238−2243.

(12) (a) Ruthven, D. M. *Principles of Adsorption and Adsorption Processes*; Wiley: New York, 1984. (b) Choudhary, V. R.; Nayak, V. S.; Choudhary, R. V. *Ind. Eng. Chem. Res.* **1997**, *36*, 1812−1818. (c) Derouane, E. G. New Aspects of Molecular Shape-Selectivity: Catalysis by Zeolite ZSM-5. In *Catalysis by Zeolites*; Imelik, B., Ed.; Elsevier: Amsterdam, 1980; pp 5−18. (c) Derouane, E. G. Molecular Shape-Selective Catalysis by Zeolites. In *Zeolite*: *Science and Technology*; Ribeiro, F. R., Ed.; Martinus, Nijhoff Publ.: The Hague, 1984; pp 347−370. (d) Derouane, E. G., Ed. *Diffusion and Shape Selective Catalysis in Zeolites*; Academic Press: New York, 1982.

Scheme 1

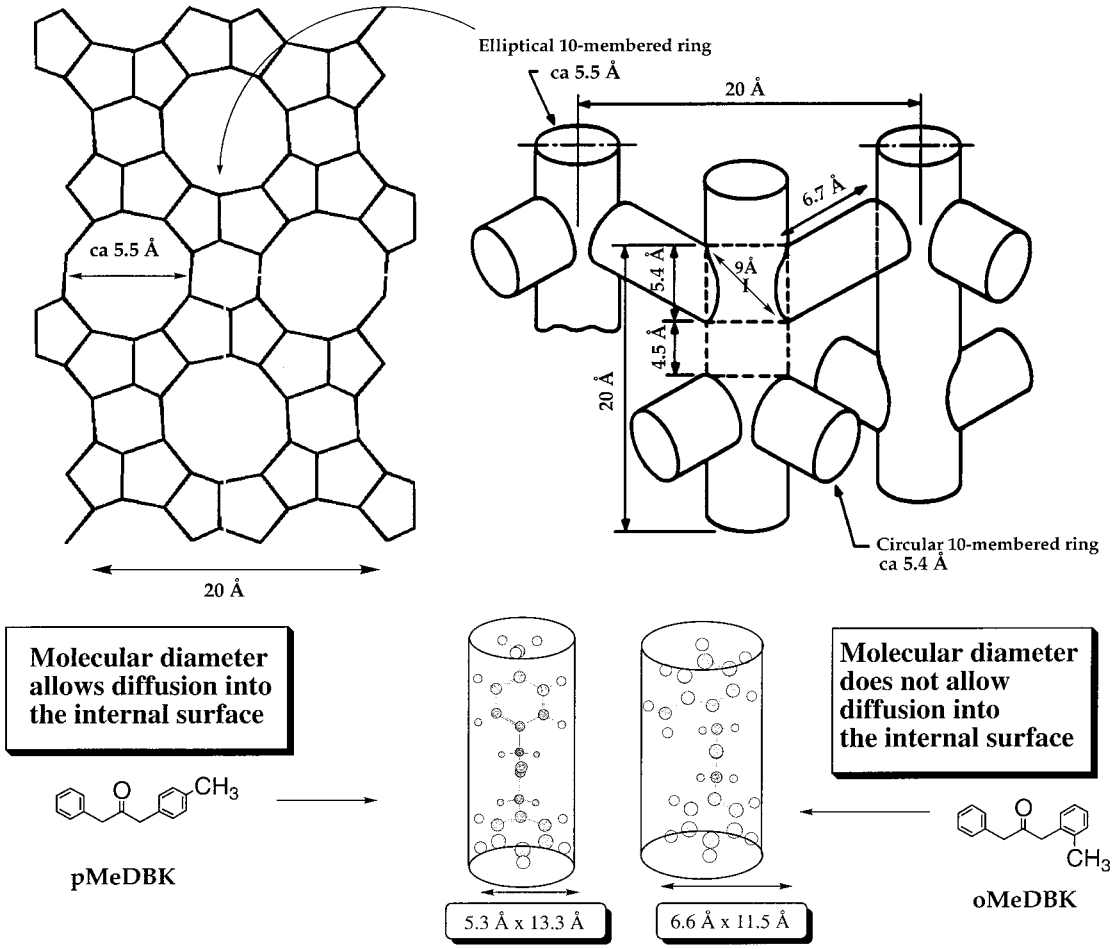

rates[12] of guests in zeolites. It has been demonstrated in previous investigations that good mass balances of radical−radical products (ca. 80−90%) can be achieved in the photolysis[13,14] of ketones@ZSM-5, ensuring that the isolated products are representative of the major portion of the photochemistry and that the zeolite framework does not react with radicals. Thus, the zeolite provides a chemically inert host for the carbon-centered radicals examined, ensuring that the persistence of the radicals will be determined by the rate of radical−radical reactions. However, we shall show that the radicals do interact with the zeolite surface and exchangeable cations and that these interactions influence the mobility and therefore the reactivity of adsorbed radicals. Radical−radical reactions on the external surface will be much more rapid than radical−radical reactions on the internal surface.[6,15,16] Thus in this study, conditions were produced that are decisive in rendering radicals persistent due to a supramolecular inhibition of radical−radical reactions on the internal surface of ZSM-5 zeolites.

A Working Paradigm for the Supramolecular Structure of Ketone@MFI Complexes. The external surface of a MFI crystal consists[11] of pores or "holes" (approximately circular ca. 5.5 Å in diameter) and "solid" framework between the holes (shown schematically in Scheme 1). The external surface of a MFI crystal possesses a surface area consisting of ca. 20−30% "holes" and ca. 70−80% "framework". The internal void space of MFI zeolites consists of channels that intersect to produce roughly spherical supercages of ca. 9 Å in diameter. For the guest ketones investigated (Chart 1), except for **1** and **1**-d_{10} (adsorbed exclusively on the internal surface until saturation of the internal surface occurs)[12] and **1**-o,o′DiMe (adsorbed exclusively on the external surface),[6a] all the guest molecules possess molecular cross sections that will allow *only partial adsorption or penetration* of a phenyl group into the holes of the external surface.

The working paradigm for the supramolecular structure of ketone@external surface complexes assumes[6] that for ortho-ring-substituted ketones (**1**-oMe and **2**-oMe) the first, more strongly bound ketone@external surface complexes formed are those for which the ketone preferentially adsorbs partially into the holes of the external surface of MFI crystals, as shown in previous investigations.[6,7,17] The preference for binding to the holes is assumed to be due to favorable dispersion interactions of an adsorbed benzene ring with the walls of the pores on the external surface. After saturation of the holes, further adsorption of ketones occurs onto the

(13) Turro, N. J.; Wan, P. *J. Am. Chem. Soc.* **1985**, *107*, 678−685.
(14) Turro, N. J.; Cheng, C. C.; Abrams, L.; Corbin, D. R. *J. Am. Chem. Soc.* **1987** *109*, 2449−2456.
(15) (a) Kelly, G.; Willsher, C. J.; Wilkinson, F.; Netto-Ferreira, J. C.; Weir, A. O. D.; Johnston, L. J.; Scaiano, J. C. *Can. J. Chem.* **1990**, *68*, 812−819. (b) Johnston, L. J.; Scaiano, J. C.; Shi, J.-L.; Siebrand, W.; Zerbetto, F. *J. Phys. Chem.* **1991**, *95*, 10018−10024.
(16) Jockusch, S.; Hirano, T.; Liu, Z.; Turro, N. J. *J. Phys. Chem. B* **2000**, *104*, 1212−1216.
(17) Turro, N. J.; Lei, X.-G.; Li, W.; Liu, Z.; McDermott, A.; Ottaviani, M. F.; Abrams, L. *J. Am. Chem. Soc.* **2000**, *122*, 11649−11659.

Scheme 2. Schematic Representation of the External Surface of ZSM-5 Zeolites[a]

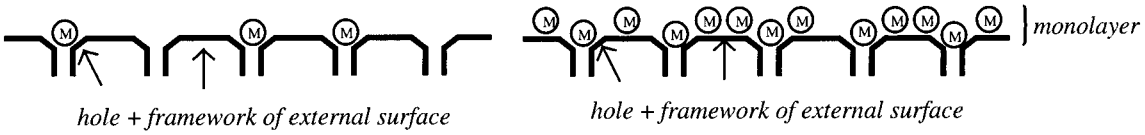

[a] The model assumes that initial binding is stronger for the holes (left), followed by binding to the framework (right) until a monolayer is formed. Left refers to "low coverage" (up to saturation of the holes); right refers to "high coverage" (beyond saturation of the holes and up to saturation of the external surface, i.e., formation of a monolayer).

Scheme 3. Schematic of Possible Siting of Ketones@ZSM-5[a]

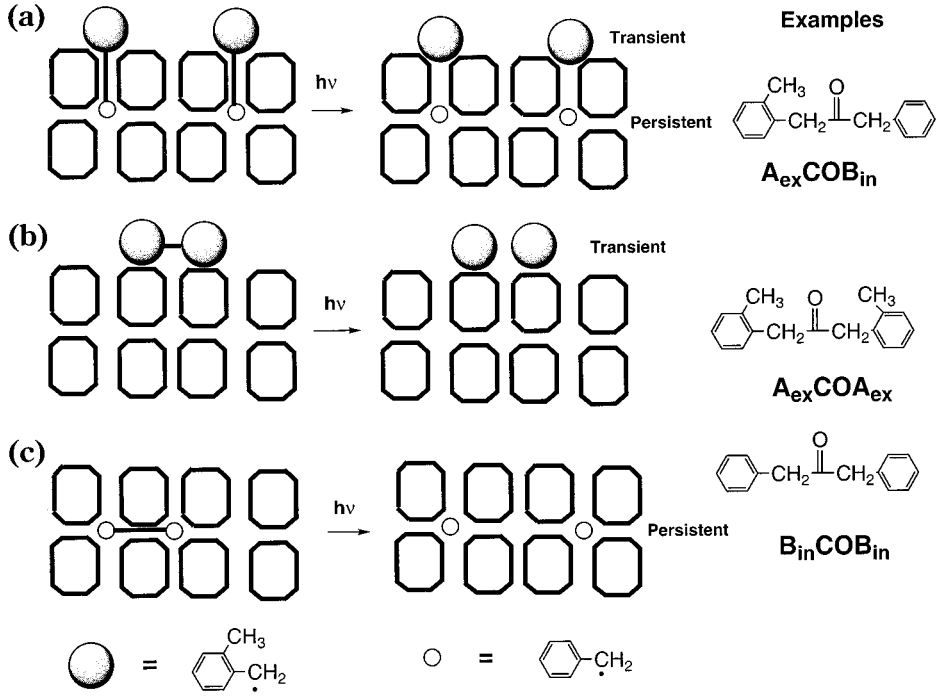

[a] See text for discussion.

framework between the holes until a monolayer is formed (Scheme 2). This paradigm predicts an important change in the supramolecular structure of the ketone@external surface complexes as a function of surface coverage: initially, ketone@hole complexes will be formed, and after all the holes are filled, ketone@framework complexes will form until a monolayer is created. It has been shown[6,17] that the behavior of the supramolecular radicals produced by the photochemistry of the two supramolecular isomers (ketone@hole and ketone@framework) is very different. The term "low coverage" will refer to situations up to saturation of the holes, and the term "high coverage" will refer to situations for which the holes are completely filled and the framework is partially or completely covered.

The Supramolecular Photochemical Paradigm. It is assumed that the primary photochemical process in all cases is α-cleavage of the ketone triplet to produce a geminate radical pair, followed by rapid decarbonylation to form a secondary radical pair.[18,19] The products of the photochemistry are determined by the supramolecular dynamic pathways available for radical−radical reactions of the secondary radical pair. These pathways are strongly controlled by (1) the initial siting of the ketone (on either the internal surface of the zeolite or at the holes and framework at the interface of the external and internal surface) and (2) the dynamics for diffusion and rotational motions of the radicals on the external and internal surface.

A Model Correlating Supramolecular Structure with Radical Persistence and Transience. A model for photolysis of ketone@hole or ketone@framework complexes[6] is shown in Scheme 3 for three limiting cases. Imagine a ketone $A_{ex}COB_{in}$ (the subscripts refer to external surface and internal surface) adsorbed on a MFI crystal [the molecular cross section of the moiety A_{ex} is assumed to be too large to allow it to pass through the hole on the external surface, and the molecular cross section of the moiety B_{in} is assumed to be small enough to fit into the hole and to diffuse into the internal surface]. Ketone **1**-o,o′DiMe and **1** (**1**-d_{10}) can be completely adsorbed into the external surface (Scheme 3b) or internal surface (Scheme 3c) until surface saturation, respectively. However, at "low coverage", the initial supramolecular structures of all of the other ketones in Chart 1 will be constrained to the interface of the zeolite crystal and will have a portion of the ketone (a phenyl group) adsorbed in the hole on the external surface; that

(18) Turro, N. J. *Modern Molecular Photochemistry*; University Science: Menlo Park, 1991.

(19) (a) Engel, P. S. *J. Am. Chem. Soc.* **1970**, *92*, 6074−6076. (b) Robbins, W. K.; Eastman, R. H. *J. Am. Chem. Soc.* **1970**, *92*, 6076−6077. (c) Robbins, W. K.; Eastman, R. H. *J. Am. Chem. Soc.* **1970**, *92*, 6077−6079.

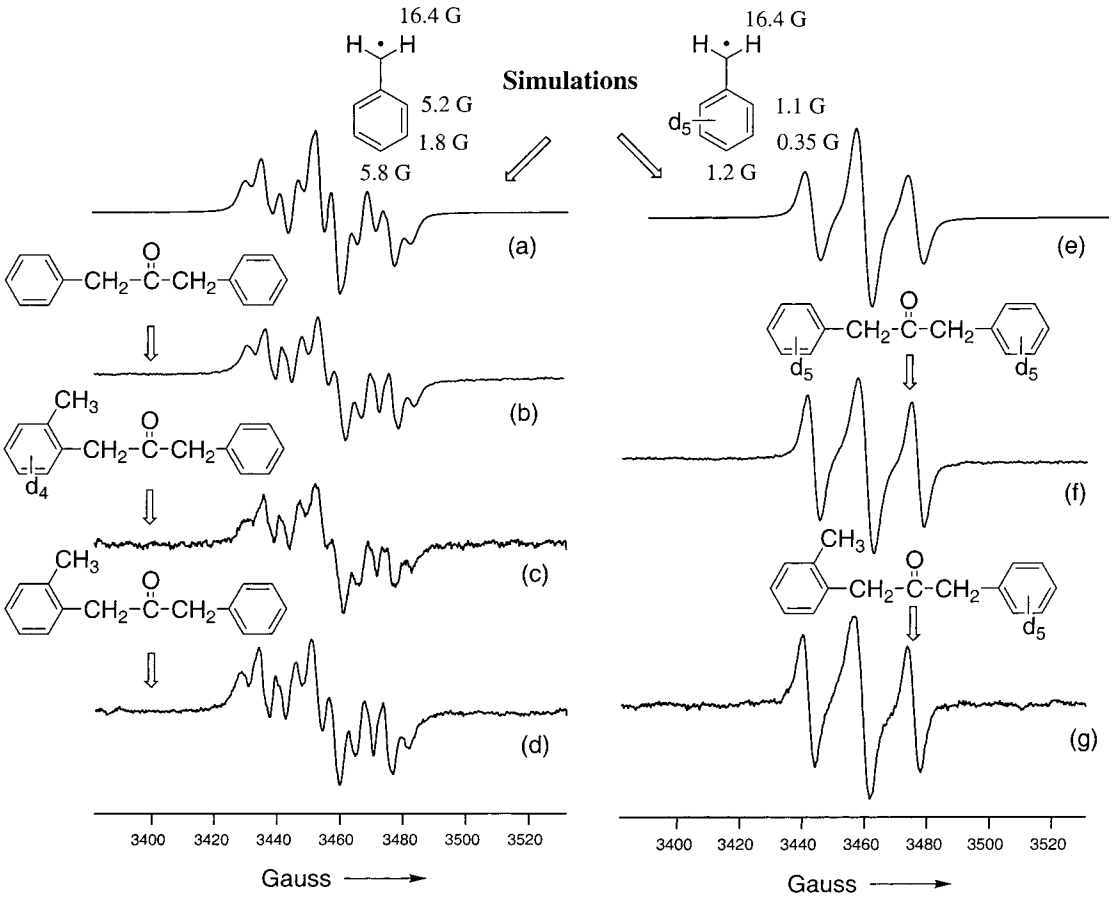

Figure 1. Steady-state CW-EPR spectra of radicals produced by the photolysis of ketones@ZSM-5: (a) simulation of B; (b) spectrum produced from photolysis of **1**; (c) spectrum produced from photolysis of **1**-oMe-d_4; (d) spectrum produced from photolysis of **1**-oMe; (e) simulation of B-d_5; (f) spectrum produced from photolysis of **1**-d_{10}; (g) spectrum produced from photolysis of **1**-oMe-d_5.

is, these ketones will be examples of a supramolecular complex, $A_{ex}COB_{in}$@hole (Scheme 3a). After all the holes are filled, at "high coverage" the ketones bind to the framework to generate a new, isomeric supramolecular complex, $A_{ex}COB_{ex}$@framework (Scheme 3b).

This paradigm suggests a number of consequences for the photolysis of $A_{ex}COB_{in}$@ZSM-5 which are experimentally testable: (1) photolysis of $A_{ex}COB_{in}$@hole (Scheme 3a, e.g., **1**-oMe) will produce, after loss of CO, two radicals, one A_{ex}, which is "directed" toward the external surface, and a second radical, B_{in}, which is "directed" toward the internal surface; (2) photolysis of A_{ex}-COB_{ex}@framework (Scheme 3b, e.g., **1**-o,o′DiMe, where A = B) will produce, after loss of CO, two radicals, A_{ex} and B_{ex}, both of which are "directed" toward the external surface; (3) photolysis of $A_{in}COB_{in}$@intersection (e.g., **1**, where A = B); (4) the radicals that are on the external surface will be able to diffuse freely and undergo rapid radical−radical reactions;[15,16] (5) the radicals that enter the internal surface will diffuse slowly and undergo radical−radical reactions that will be inhibited to some extent by supramolecular steric effects within the supercages of the internal surface; (6) the radicals undergoing rapid radical−radical reactions on the external surface will tend to be transient, and those that migrate into the internal surface and undergo slower radical−radical reactions on the internal surface will tend to be persistent;[7] (7) there will be a coverage dependence of the yield of persistent radicals and the products of radical−radical reactions.[6] The coverage dependences will correlate with the filling of the holes on the external surface.

It will be shown directly by EPR spectroscopy that the persistent radicals@ZSM-5 are quite reactive toward small molecules such as oxygen and nitric oxide that can easily diffuse throughout the zeolite surface. In addition, product analysis demonstrates that radical−radical reactions do occur and that the products of these reactions depend strongly on the supramolecular structures and dynamics of the systems investigated.

Results

Steady-State EPR Produced by Photolysis of Ketones@ZSM-5. The ketones **1**, **1**-d_{10}, **1**-oMe, **1**-oMe-d_4, and **1**-oMe-d_5 (Chart 1) were adsorbed (ca. 1 wt %/wt) on ZSM-5 to form supramolecular complexes termed **1**@ZSM-5, **1**-d_{10}@ZSM-5, **1**-oMe@ZSM-5, **1**-oMe-d_4@ZSM-5, and **1**-oMe-d_5@ZSM-5, respectively. Photolysis of sealed vacuum-degassed samples of **1**@ZSM-5, **1**-oMe@ZSM-5, and **1**-oMe-d_4@ZSM-5 produced experimentally indistinguishable EPR spectra (Figure 1, left). In a typical experiment, samples were photolyzed for ca. 7 min under comparable conditions. The observed spectra produced from photolysis of **1**, **1**-oMe, and **1**-oMe-d_4 are assigned to a single species, the benzyl radical (B, Chart 2), based on spectral simulation (Figure 1, left top) and alternate methods of preparation (Figure 1).

Photolysis of sealed vacuum-degassed samples of **1**-d_{10}@ZSM-5 and **1**-oMe-d_5@ZSM-5 produced experimen-

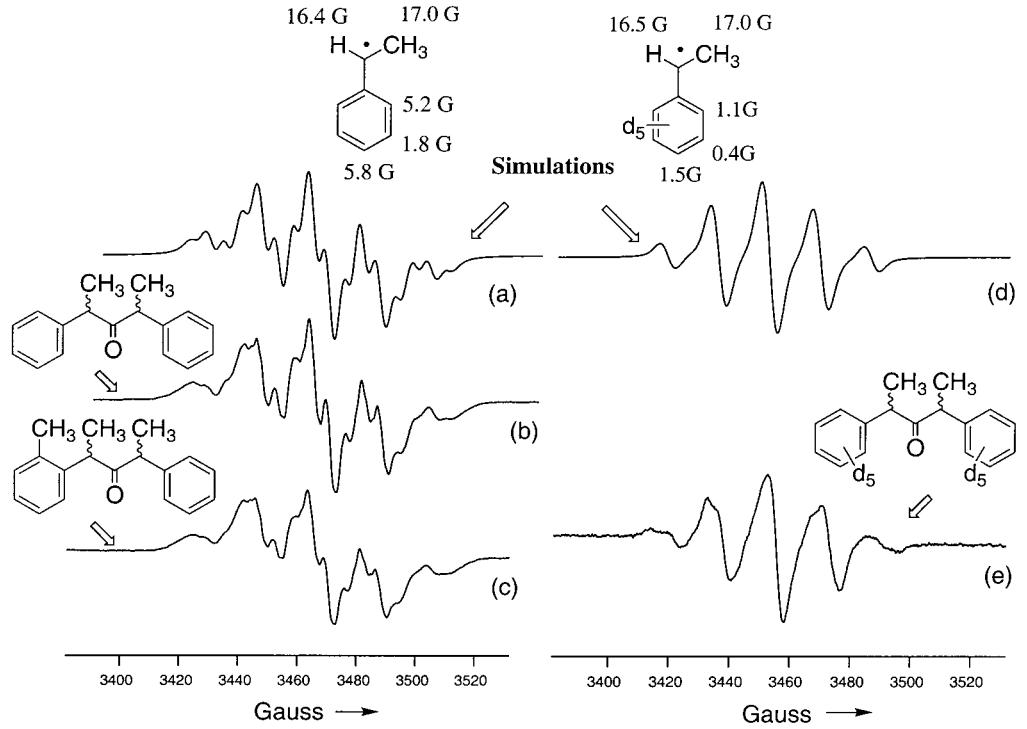

Figure 2. Steady-state CW-EPR spectra of radicals produced by the photolysis of ketones@ZSM-5: (a) simulation of α-MeB; (b) spectrum produced from photolysis of **2**; (c) spectrum produced from photolysis of **2**-oMe; (d) simulation of α-Me-B-d_5; (e) spectrum produced from photolysis of **2**-d_{10}.

Chart 2. Structures of Radicals Discussed in This Report

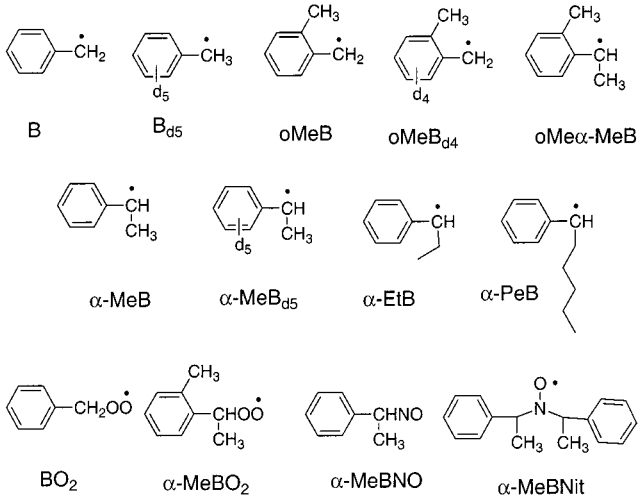

tally indistinguishable steady-state EPR spectra (Figure 1, right). These spectra are assigned to a single species, the ring deuterated benzyl radical (B_{d5}, Chart 2), based on spectral simulation (Figure 1, right top) and alternate methods of preparation (Figure 1). All of the EPR spectra shown in Figure 1 were reproducible at room temperature and possessed "half-lives" on the order of 10 min. The results convincingly demonstrate that oMeB and oMeB-d_4 (Chart 2), produced by photolysis of **1**-oMe and **1**-oMe-d_4, are not persistent on the time scale of the measurements, whereas the benzyl radicals produced by the photolysis of **1** (**1**-d_5) or **1**-oMe (**1**-oMe-d_4) are persistent (eqs 1a and 1b). It is important to note that the persistent radical (B) has a kinetic cross section similar to *p*-xylene (which can be adsorbed in the internal surface of ZSM-5 at room temperature), whereas the transient radical (oMeB) has a kinetic cross section similar to *o*-xylene (which cannot be adsorbed into the internal surface of ZSM-5 zeolites at room temperature).[11d,e] Photolysis of **1**-o,o′DiMe (Chart 1) serves as a control for persistent radicals. Photolysis of **1**-o,o′DiMe@ZSM-5 complexes, as predicted by the model, leads to no persistent EPR signals of oMeB within the experimental uncertainty (results not shown), demonstrating that the oMB radicals are transient (eq 1c).

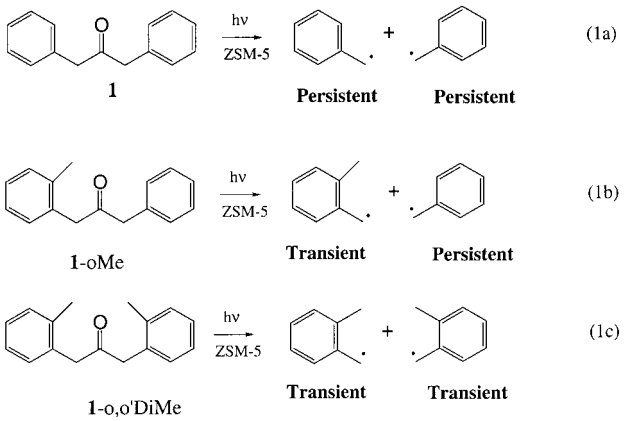

The supramolecular complexes **2**@ZSM-5, **2**-oMe@ZSM-5, and **2**-d_{10}@ZSM-5 were photolyzed under the conditions described above and analyzed by steady-state EPR. Photolysis of sealed vacuum-degassed samples of **2**@ZSM-5 and **2**-oMe@ZSM-5 produced an experimentally indistinguishable EPR spectrum (Figure 2, left), assigned to a single species, the α-methyl benzyl radical (α-MeB, Chart 2), based on spectral simulation (Figure 2, top left) and an alternate method of preparation (Figure 2).

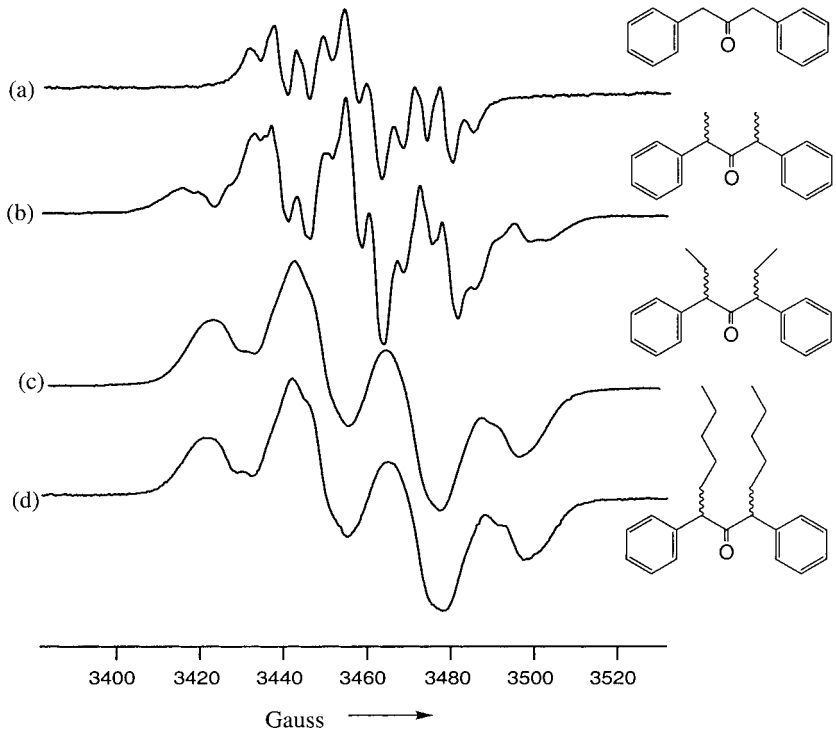

Figure 3. Steady-state CW-EPR spectra of radicals produced by the photolysis of ketones@ZSM-5: (a) spectrum produced by the photolysis of **1**; (b) spectrum produced from photolysis of **2**; (c) spectrum produced from photolysis of **3**; (d) spectrum produced from photolysis of **4**.

Photolysis of sealed vacuum-degassed samples of **2**-d_{10}@ZSM-5 produced the EPR spectrum shown in Figure 2, right. This spectrum is assigned to a single species, the ring-deuterated α-methyl benzyl radical, based on spectral simulation (Figure 2, right top). The EPR spectra shown in Figure 2 were persistent at room temperature with "half-lives" on the order of 60 min. The results demonstrate that the oMe-substituted radicals (oMeB, Chart 2) produced from photolysis of **2**-oMe@ZSM-5 are not persistent on the time scale of the measurements, whereas the α-MeB radicals are persistent (eqs 2a and 2b).

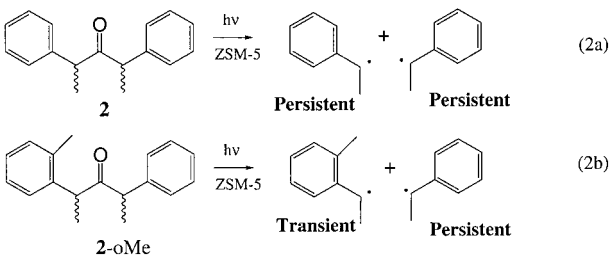

Influence of α-Alkyl Substituents on the EPR Produced by Photolysis of α,α′-Dialkyl Dibenzyl Ketones@ZSM-5. The effect of the length of the α-alkyl chain on the EPR spectra produced on photolysis of α,α′-dialkyl ketones was investigated for the α,α′-dialkyl dibenzyl ketones **3** and **4** adsorbed on ZSM-5. Figure 3 shows the EPR spectra produced upon photolysis of samples of **3**@ZSM-5 and **4**@ZSM-5, with the spectra resulting from photolysis of **1**@ZSM-5 and **2**@ZSM-5 included for comparison. In each case the dominant species that carries the EPR signal is assigned to an α-alkyl benzyl radical. However, as the alkyl increases in size, a significant broadening of the EPR signals occurs compared to those observed upon photolysis of **2**@ZSM-5 (and **1**@ZSM-5). In addition, the intensity and persistence of the α-alkyl B radical increases (results not shown) with the increasing size of the alkyl group, i.e., α-PeB > α-EtB > α-MeB > B.

Scavenging of Benzyl and α-Methyl Benzyl Radicals by Molecular Oxygen. The EPR spectra of the benzyl radical produced from photolysis of **1**@ZSM-5 or **1**-oMe@ZSM-5 are transformed into the EPR spectra of different persistent radicals by addition of air (Figure 4, left). Similarly, the EPR spectra of the α-methyl benzyl radical produced from photolysis of **2**@ZSM-5 and **2**-oMe@ZSM-5 are transformed to the EPR spectra of different persistent radicals (Figure 4, right) that are distinct from those produced from photolysis of **1**@ZSM-5 or **1**-oMe@ZSM-5.

The EPR spectra produced by addition of air to photolyzed samples are assigned to peroxy radicals (eqs 3 and 4) based on computer simulation of a powder

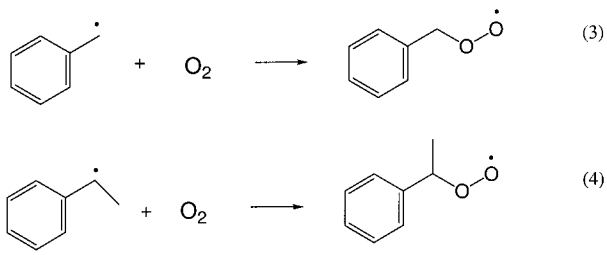

spectrum of a peroxy radical and on comparison with the EPR spectrum obtained from photolysis of cumene peroxy radical in a solid matrix.[20,21] The relative amounts of

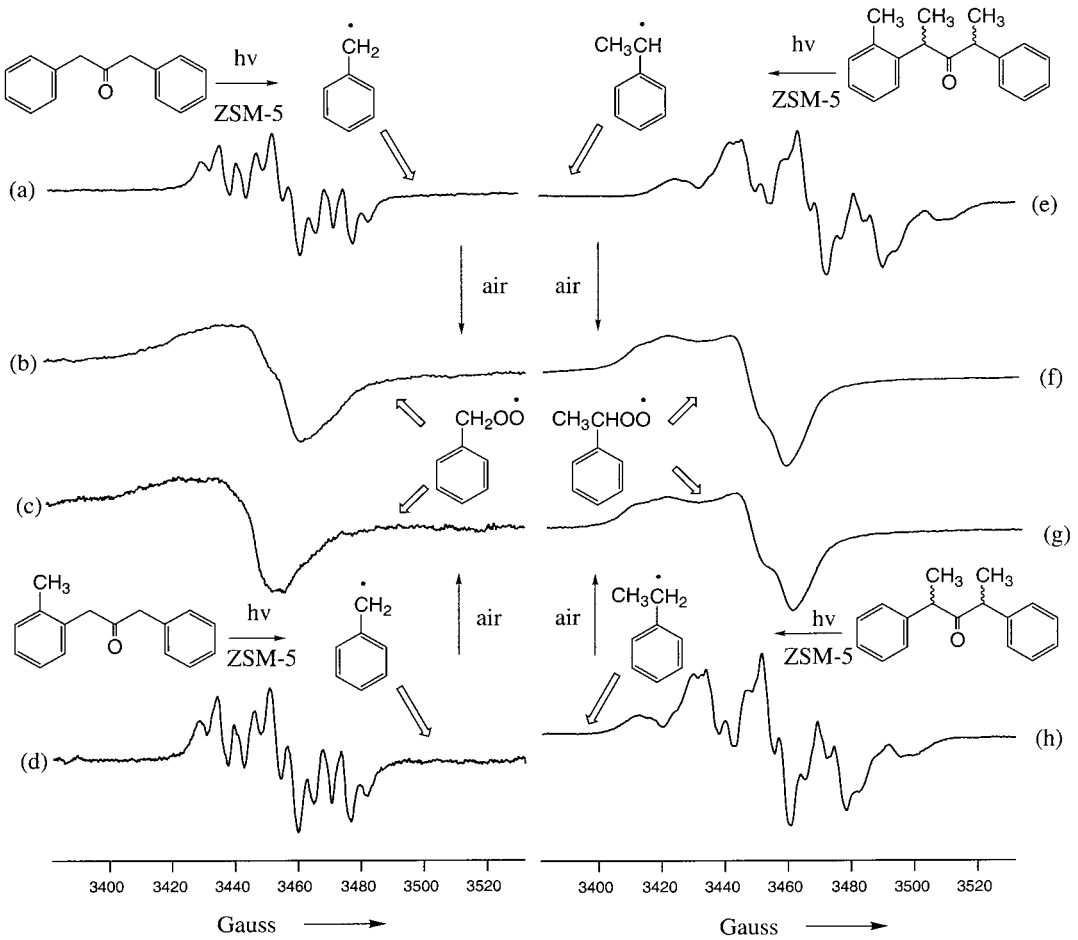

Figure 4. Effect of addition of air to the steady-state CW-EPR spectra of radicals produced by the photolysis of ketones@ZSM-5: (a, d, e, and h) spectra produced by photolysis of **1**, **1**-oMe, **2**-oMe, and **2**, respectively; (b, c, f, and g) spectra produced upon addition of air to the samples corresponding to a, d, e, and h, respectively.

radicals (determined by double integration of the spectra) were essentially identical before and after aeration of the samples, indicating that the persistent benzyl and α-methyl benzyl radicals are converted to persistent peroxy radicals in high yield. The fact that the spectra of the peroxy radicals correspond to those expected for a rigidly held radical indicates that the peroxy radicals are very restricted in motion.Vacuum removal of the oxygen in the samples did not affect the peroxy radical spectrum, indicating that the reaction of the benzyl and α-methyl benzyl radicals with oxygen is irreversible.[22]

Scavenging of α-Methyl Benzyl Radicals by Nitric Oxide. Exposure of a photolyzed vacuum-degassed sample of **1**@ZSM-5 or **2**@ZSM-5 to nitric oxide resulted in the complete disappearance[23] of the benzyl and α-methyl benzyl radical EPR spectrum, respectively. A representative example is shown in Figure 5 for the addition of nitric oxide to irradiated samples of **2**@ZSM-5. Addition of nitric oxide (ca. 2 Torr, molar ratio of ketone to NO = 2) caused the entire EPR spectrum of the α-methyl benzyl radical to disappear (Figure 5, middle). Further irradiation of a sealed sample containing nitric oxide resulted in the appearance of a new EPR spectrum which could be assigned by computer simulation to that of a nitroxide shown in eq 5 (Figure 5, top).

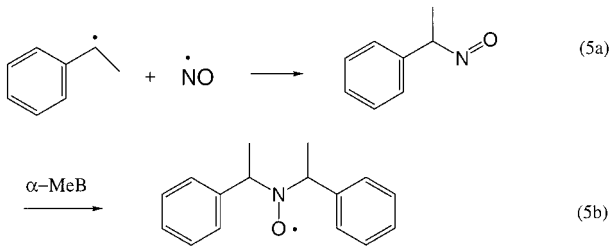

Product Analysis of the Photolysis as a Function of Loading. The major product produced by photolysis of **1**@ZSM-5 was found to be 1,2-diphenylethane (eq 6) and is independent of loading in the range of 0.1−5% (wt/wt). However, the products produced from photolysis of **2**@ZSM-5 are strongly dependent on loading in the range of 0.1−5%. For loadings in the range from ca. 0.1 to 1% the ratio of disproportionation (eq 7) to combination (eq 8) is ca. 3−5 (values decreasing with increasing coverage), and for loadings in the range from ca. 1−5% the ratio of disproportionation to combination is ca. 0.2−0.8 (decreasing with increasing coverage). In solution, the ratio of disproportionation to combination is ca. 0.1 for photolysis

(20) Schlick, S.; Kevan, L. *J. Phys. Chem.* **1979**, *83*, 3424−3429.
(21) Kevan, L.; Schlick, S. *J. Phys. Chem.* **1986**, *90*, 1998−2007.
(22) Hirano, T.; Li, W.; Abrams, L.; Krusic, P. J.; Ottaviani, M. F.; Turro, N. J. *J. Am. Chem. Soc.* **1999**, *121*, 7170−7171.
(23) For examples of trapping of radicals with NO in solution see: (a) Maruthanmuthu, P.; Scaiano, J. C. *J. Phys. Chem.* **1978**, *82*, 1588−1591. (b) Gyor, M.; Rochenbauer, A.; Tudos, F. *Tetrahedron Lett.* **1986**, *32*, 3759−3762.

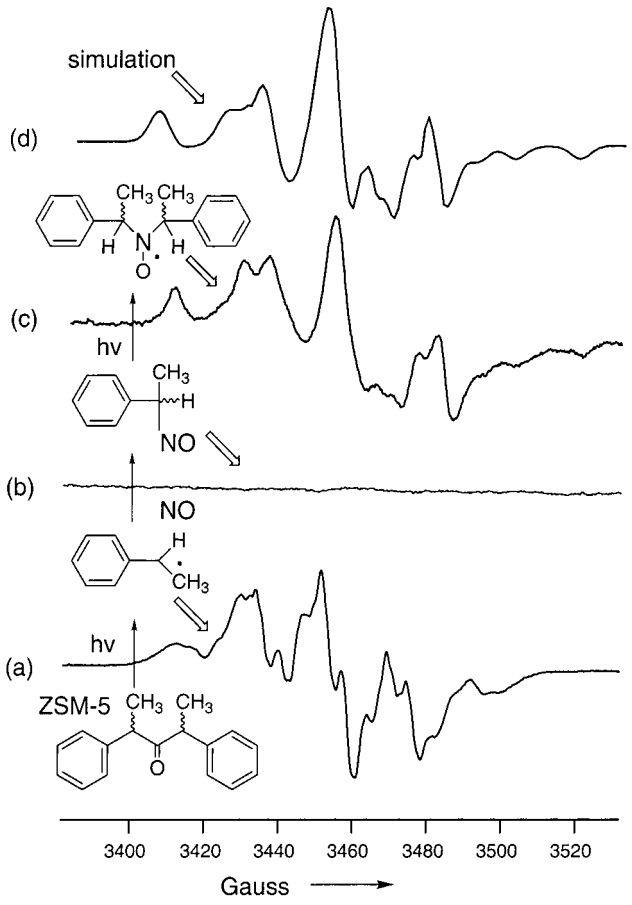

Figure 5. Effect of the addition of nitric oxide to the steady-state CW-EPR spectra of radicals produced by the photolysis of **2**@ZSM-5: (a) spectrum produced from photolysis of **2**; (b) spectrum produced upon addition of nitric acid; (c) spectrum produced upon further photolysis of sample after addition of nitric oxide; (d) simulated spectrum of the nitroxide α-MeBNit.

of **2**, i.e., a value comparable to that for the higher loadings of **2**@ZSM-5.

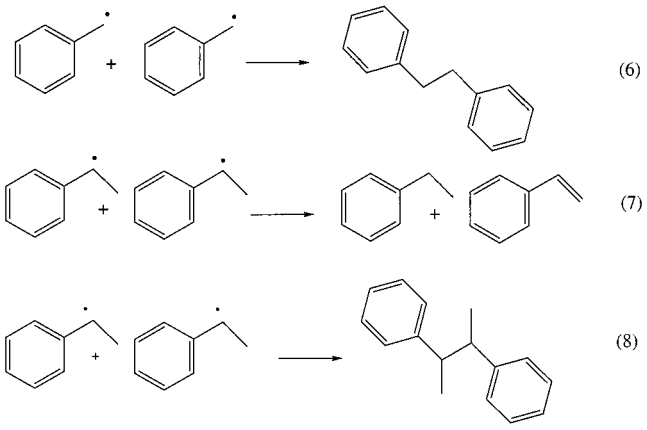

Discussion

The molecular photochemistry of the dibenzyl ketone family of ketones has been well established.[18,19] In common organic solvents after photochemical excitation, the initially produced singlet excited state of **1** is transformed nearly quantitatively to the triplet state and undergoes rapid (k_α ca. 10^9 s^{-1}) primary photochemical α-cleavage, followed by rapid (k_{-CO} ca. 10^7 s^{-1}) secondary thermal decarbonylation[24] to form free benzyl radicals. For both the benzyl radicals (produced from photolysis of **1**) and the α-methyl benzyl radicals (produced from photolysis of **2**) radical−radical recombination proceeds at close to the rate of diffusion and leads to diphenyl ethanes (eqs 1 and 6) as the dominant products in ca. 90% yield.[25]

The primary supramolecular photochemistry of **1** and **2** adsorbed on zeolites is assumed to be identical to the molecular photochemistry (α-cleavage from the triplet followed by rapid decarbonylation). However, the reactions of the secondary geminate benzyl and α-methyl benzyl radical produced are strongly influenced by the supramolecular structure and dynamics of the radicals@zeolite complexes. We now analyze the initial supramolecular structure of the ketone@ZSM-5 complexes and then interpret the experimental result in terms of the supramolecular model presented above (Scheme 3).

Transient and Persistent Radicals Produced by Photolysis of Ketone@ZSM-5 Complexes. Of the ketones investigated (Chart 1), only **1** and **1**-d_{10} (minimum molecular cross sections <5.5 Å) possess a kinetic molecular cross section that allows ready access to the internal surface at room temperature, since the holes (pores) on the external surface have a "void" cross section of ca. 5.5 Å (Scheme 1). The ketones **1**-oMe, **2**, and **2**-oMe (minimum molecular cross sections >5.5 Å) are too large to enter the internal surface by sieving through the pores on the external surface. However, one of the phenyl groups of the latter ketones can be adsorbed into a pore on the external surface. If such supramolecular structures are formed, then the part of the ketone molecule that is adsorbed in the pore will be in good position to be adsorbed into the *internal* surface after photochemically induced α-cleavage; the other larger moiety of the molecule will be in good position to be adsorbed on the *external* surface after photochemically induced α-cleavage. Finally, **1**-o,o′DiMe possesses a structure that prevents the insertion of either ring into the pores on the external surface. It is important to note that the internal surface of ZSM-5 zeolites possesses ca. 500 m^2/g of internal surface and ca. 10 m^2/g of external surface. However, adsorption on the huge internal surface can only occur for molecules or reactive intermediates whose size/shape characteristics allow diffusion into the internal surface. Scheme 3 shows the supramolecular structural paradigm used to interpret the results. At loadings on the order of ca. 0.5% or less, all of the ketones except **1**, **1**-d_{10}, and **1**-o,o′diMe are adsorbed in or near the holes of the external surface, with a benzyl (or α-methyl benzyl) moiety associated with the hole on the external surface (Scheme 3a). On the other hand, **1** will be primarily adsorbed on the internal surface (Scheme 3c), plausibly at the spherical intersections which possess diameters of ca. 9 Å, and **1**-o,o′diMe will be adsorbed exclusively on the external surface (Scheme 3b).[26] Photolysis of **1**@ZSM-5 produces, after decarbonylation, secondary geminate radical pairs which either recombine to form 1,2-diphenyl-

(24) (a) Lunazzi, L.; Ingold, K. U.; Scaiano, J. C. *J. Phys. Chem.* **1983**, *87*, 529−530. (b) Turro, N. J.; Gould, I. R.; Baretz, B. H. *J. Phys. Chem.* **1983**, *87*, 531−532. (c) Gould, I. R.; Baretz, B. H.; Turro, N. J. *J. Phys. Chem.* **1987**, *91*, 925−929.

(25) (a) Baretz, B. H.; Turro, N. J. *J. Am. Chem. Soc.* **1983**, *105*, 1309−1316. (b) Ghatlia, N. D.; Turro, N. J. *J. Photochem. Photobiol. A: Chem.* **1991**, *57*, 7−19.

ethane (eq 6) or diffuse apart to form free benzyl radicals. The geminate coupling of benzyl radicals occurs on a very short time scale, and the radicals that combine geminately are transient and are not detected by steady-state EPR. The benzyl radicals that diffuse apart become free radicals, some of which become persistent and are detected by steady-state EPR. This feature of the model is consistent with the observation that the cage effect for secondary radical recombination is ca. 60−70% for **1**@ZSM-5.[27]

Thus, the interpretation of the EPR spectra produced from photolysis of **1**@ZSM-5 (Figure 1) is that for each system the spectra are due to persistent benzyl radicals that have escaped from the cage in the zeolite internal surface in which they were produced. The persistence (lifetime) of these radicals is determined by the rate of radical−radical combination reactions. The rate-limiting feature of radical−radical reactions may be the time scale for a pair of diffusing free radicals to find each other at an intersection as they percolate through the porous internal surface of the zeolite (supramolecular diffusion-controlled combination). Since geminate recombination of benzyl radicals has been shown to occur relatively efficiently in the supercages at the intersections,[14] it is likely that the rate-limiting feature is related to diffusionally controlled limited recombination on the internal surface. Other mechanistic possibilities can be envisioned (e.g., diffusion to and recombination on the external surface) but are considered less likely. Thus, we conclude that the lifetime of the persistent benzyl radicals is limited by the rate at which radicals diffuse together and encounter at an intersection of the internal surface and that the reaction mechanism is analogous to diffusion-controlled reaction of radicals in fluid solution.

The situation for **1**-o,o′DiMe@ZSM-5 is quite different, as there is no significant EPR signal observed upon photolysis. This is the expected result for the situation in Scheme 3b for which the radicals are produced on the external surface and for which the size of the radicals is too large to allow kinetic entry to the internal surface. In this case, rapid diffusion and radical−radical reactions occur on the external surface. In contrast to the situation for **1**@ZSM-5 and **1**-o,o′DiMe, the ketones in the **1**-oMe@ZSM-5, **2**@ZSM-5, and **2**-oMe@ZSM-5 complexes are not adsorbed on the internal surface, but are mainly adsorbed on the framework or pore system on the external surface. Although photolysis of **1**-oMe@ZSM-5, **2**@ZSM-5, and **2**-oMe@ZSM-5 results in α-cleavage and decarbonylation, the resulting structure of the resulting radical pair is supramolecularly asymmetric, since one radical is formed adsorbed in a hole and the other radical is formed on the external surface (Scheme 3a). The radicals formed on the external surface are able to diffuse rapidly on the external surface, mainly encounter other radicals of the same type, and undergo rapid, probably diffusion-controlled radical−radical combination reactions.[15,16] These radicals will be transient, and their EPR spectra will not be observed on the time scale of seconds. It should be noted in passing that in favorable cases (diphenyl methyl) transient radicals adsorbed on the external surface can be observed by laser flash photolysis methods and that the radicals decay on a microsecond time scale.[15,16] The radicals formed in the pores will tend to diffuse into the internal surface and become persistent by the definition employed in this study.

With this supramolecular structural and dynamic model in mind, we now consider the implications on the EPR spectra produced by photolysis of **1**@ZSM-5 and **1**-oMe@ZSM-5 (Figure 1). The observed spectra are assigned to persistent benzyl radicals based on the good fit of the simulated spectra to the experimental spectra and on the fact that the same spectrum is produced from two precursors. The absence of a contribution from the ortho-methyl benzyl radical (which has a distinctly different EPR spectrum from the benzyl radical)[17] is mechanistically significant, since it confirms the supramolecular structural assumption that the ortho-methyl benzyl moiety (oMeB, Chart 2) cannot enter the internal surface and become persistent. Although ortho-methyl benzyl radicals are produced (as demonstrated by product analysis),[14] they rapidly diffuse on the external surface, undergo recombination reactions, and are not persistent on the time scale of seconds or longer, and their steady-state EPR spectrum is not observed.

The lifetime of the B radicals produced by photolysis of **1**@ZSM-5 or **1**-oMe@ZSM-5 is qualitatively the shortest of the radicals investigated. This is attributed to the faster diffusional dynamics of the B radical compared to the other radicals investigated and to the smaller cross section of the coupling product formed by combination of B radicals at an intersection (eq 6). We speculate that of all the persistent radicals investigated, only B can undergo radical−radical combination at close to the rate of diffusion on the internal surface; that is, there is a minimal supramolecular steric effect on the combination of two B radicals in a ZSM-5 intersection.

The EPR produced by photolysis of **2**@ZSM-5 and **2**-oMe@ZSM-5 (Figure 2) are assigned to the α-methyl benzyl radical based on the good fit of the simulated spectra to the experimental spectra and on the fact that the same spectrum is produced from two precursors. As in the case of photolysis of **1**-oMe@ZSM-5, the absence of a contribution of the oMeα-MeB radical from the photolysis of **2**-oMe@ZSM-5 is significant and demonstrates that, although the α-MeB radical can diffuse into the internal surface and become persistent, oMeα-MeB cannot. The latter radicals are produced on the external surface where they diffuse and react rapidly and are transient, as is the case for the o-MeB radicals produced from photolysis of **1**-oMe and **1**-o,o′DiMe.

In summary, the EPR results of Figures 1 and 2 are completely consistent with the supramolecular model (Scheme 3), which predicts that benzyl and α-methyl benzene radicals that are able to be adsorbed in the internal surface can become persistent and are responsible for the observed EPR spectra, but the oMe-substituted radicals (oMeB and oMeα-MeB) are adsorbed only on the external surface and therefore are transient.

Influence of α-Alkyl Substituent on the EPR Spectrum. The variation of the α-alkyl substituent has three effects on the EPR spectra (in addition to the specific changes of hyperfine couplings due to changes

(26) We note at this point that if the exact supramolecular structure does not have the phenyl group protruding in the hole, it must have characteristics that are equivalent to this structure. In particular, the actual structure must be stoichiometrically related to the number of holes, such that the smaller moiety of the molecule tends to be adsorbed into the internal surface. One could imagine, for example, an alternate structure that is bonded near a hole through SiOH bonds and for which the proximity to the hole enhances the probability of adsorption into the internal surface, which is only possible for the smaller fragments produced by photolysis.

(27) Lei, X.-G. Unpublished results.

in the coupled protons on going from a CH_3 substituent to a CH_2R substituent), as shown in Figure 3: the line widths, the half-lives (not shown), and the intensity of the spectra (not shown). The trend is that, as the size of the alkyl substituent increases, the line width, the half-life, and the intensity of the spectra increase. These observations are consistent with a dominating steric effect on the motion and diffusion of the radicals. As the alkyl group gets larger, the steric effects increase, leading to an inhibition of the rotational and diffusional motion of the persistent radicals. The inhibition of rotation results in broader lines; the inhibition of diffusion results in slower radical−radical reaction, which, in turn, leads to a higher persistent radical concentration and a stronger signal and half-lives. These conclusions are consistent with measurements of the rates of diffusion of molecules such as toluene, ethylbenzene, and *n*-propylbenzene in ZSM-5.[12b]

Oxygen Scavenging of Persistent Radicals. The addition of air to samples containing persistent benzyl radicals or persistent α-methyl benzyl radicals (Figure 4, eqs 3 and 4) shows that both types of radicals react with oxygen to produce persistent peroxy radicals; that is, the EPR spectrum of the carbon-centered radical is transformed essentially quantitatively into the EPR of the peroxy radical. These results are consistent with earlier investigations of the diphenyl methyl radical.[22] However, it was found in the case of the diphenyl methyl radical that the addition of oxygen was reversible at room temperature. In the case of the benzyl and α-methyl benzyl radicals, the reaction with oxygen is irreversible at room temperature. These results demonstrate the ability to perform reactions with the persistent radicals and to track the reactions in situ by steady-state EPR spectroscopy.

Nitric Oxide Scavenging of Persistent Radicals. The reaction of persistent radicals adsorbed on zeolites with NO is quite remarkable (Figure 5, eq 5). Initial addition of NO results in complete disappearance of the EPR signal. Photolysis of the sample after addition of NO (ca. 2 Torr) causes the creation of a strong EPR signal, comparable in intensity to that of the original persistent radical signal. From simulations the new EPR is assigned to a nitroxide radical (eq 5), formed by addition of an α-methyl benzyl radical to the nitroso compound formed by scavenging.[23] This is an important result, because it confirms the conclusion that diffusion of α-methyl benzyl radicals occurs mainly within the internal surface and is an example of scavenging of persistent radicals by a trap that is situated on the internal rather than on the external surface. This conclusion is supported by product distribution studies discussed in the next section.

Products from Photolysis of 1 and 2. Photolysis of **1** produces 1,2-diphenylethane (eq 6) as the exclusive product. The formation of 1,2-diphenylethane as the exclusive product from radical−radical combination reactions of B radicals (eq 6) is not surprising, because the size (ca. 9 Å, Scheme 1) of the intersection of the ZSM-5 internal surface allows the product to fit comfortably. This feature and the experimental EPR have led to the conclusion that recombination of B radicals is probably at a rate close to diffusion controlled in the internal surface. In this case, persistence is limited by the rate of diffusion.

Computer simulations suggest that the molecular cross section of the coupling product of α-methyl benzyl radicals (eq 8) is so large that it will possess a high "strain" energy when adsorbed in the intersections of the internal surface of MFI zeolites. As a result, radical−radical combination, essentially the exclusive reaction of α-methyl benzyl radicals in solution,[25] is expected to be strongly inhibited by this supramolecular steric effect. However, some radical−radical reactions must occur, since the adsorbed α-methyl benzyl radicals do disappear over a period of hours. Thus, the α-methyl benzyl radicals are persistent because they are adsorbed into the internal surface and because combination reactions are strongly inhibited due to supramolecular steric effects to combination. In contrast with the case of B radicals, which undergo diffusion-controlled combination, α-MeB radicals undergo reaction (or conformation)-limited disproportionation. The high energy barrier for radical−radical combination reaction of α-MeB radicals compared to the comparable reaction of B radicals is confirmed by computer simulation.

Examination of the product distribution from the photolysis of **2**@ZSM-5 as a function of loading provides insight into the reaction responsible for removal of the persistent radicals. At lower loadings, the main products are styrene and ethylbenzene (eq 7), structures expected from radical−radical disproportionation, whereas at high loadings 2,3-diphenylbutane (eq 8), the result of radical−radical combination, is the major product. At low loading of 0.3%, the ratio of disproportionation to combination is 3, whereas at a high loading of 5% the ratio of disproportionation to combination (0.3) is comparable to the value for photolysis of **2** in benzene.

These results on product distributions are interpreted as follows. At low loadings, molecules of **2** are mainly adsorbed in the holes on the external surface and after photolysis some of the α-MeB radicals generated are sieved into the internal surface. These radicals are more persistent than are B radicals, because radical−radical reactions of α-MeB are strongly inhibited in the internal surface. However, the inhibition to radical−radical disproportionation of α-MeB radicals is evidently less than that for radical−radical combination. This is plausible since the disproportionation reaction produces two molecules and does not produce a product that is too large to fit in the zeolite intersection. Thus, the steric requirements for disproportionation are less than those for combination.

At high loadings, molecules of **2** are adsorbed in all of the holes and also on the framework between the holes and in multilayers. Thus, photolysis of **2**@ZSM-5 at high loadings produces a significant number of radicals that cannot enter the internal surface, because the holes are plugged by ketone molecules. These radicals, however, can diffuse on the external surface, encounter, and undergo combination reactions without steric inhibition.

Finally, product analysis from the photolysis of **1**-o,o′DiMe@ZSM-5 results in a product distribution for which the coupling of oMeα−MeB radicals dominates. This result demonstrates that these radicals do not enter the internal surface and react dominantly on the external surface.

Conclusions

The photolysis of the supramolecular complexes formed by adsorption of the ketones shown in Chart 1 onto ZSM-5 produces persistent radicals (Figures 1−3). The

detailed features of the EPR spectra depend on the loading and the molecular structure of the guest ketone. These features are predictable on the basis of the initial supramolecular structure, ketone@ZSM-5, which undergoes photolysis (Scheme 3), and on the dynamics and reactions of radicals@ZSM-5 that result from photolysis. These initial supermolecular structures determine the supramolecular structures of the carbon-centered radicals produced by photolysis. Radicals that are constrained to the external surface (e.g., oMeB, oMe, α-MeB, Chart 2) diffuse on the external surface, undergo rapid radical−radical reactions, are transient, and are not observed by steady-state EPR. Radicals that are generated in the internal surface or that diffuse into the internal surface undergo slow radical−radical reactions and are persistent and observed by steady-state EPR.

The persistent radicals react with oxygen to form persistent peroxy radicals. Persistent radicals react with nitric oxide to form diamagnetic nitroso compounds that can undergo further reaction with radicals to form nitroxides.

The products produced from persistent radicals on the internal surface are determined by steric constraints or radical−radical reactions in the supercages of the internal surface. Benzyl radicals are small enough to undergo radical−radical recombination in the supercages within a time frame of minutes. On the other hand, α-methyl benzyl radicals are too large to undergo radical−radical combination in a supercage and instead undergo the sterically less demanding radical−radical disproportionation on the time scale of hours.

From time-resolved laser flash experiments it has been shown that radical−radical recombination on the external surface of ZSM-5 occurs in microseconds,[15,16] a time scale typical of radical−radical reactions in solution. Thus, the rates of radical−radical reactions on the external surface (microseconds) can be orders of magnitude faster than reaction of the same radicals on the internal surface (minutes to hours), demonstrating the strong control of supramolecular steric effects on the dynamics of radical−radical reactivity.

Experimental Section

General Methods. Gas chromatography was performed on a HP5890 gas chromatograph equipped with a 29 mHP-1 capillary column and FID detector. ^{1}H NMR (300 MHz and 400 MHz) and ^{13}C NMR (75 and 100 MHz) were recorded on a Bruker NMR spectrometer using $CDCl_3$ (TMS) as solvent. GC−MS (EI) spectra were recorded on a HP5792 mass selective detector, connected to a HP5890II gas chromatograph with a 20 mHP-5 capillary column. The MS detector was calibrated with perfluorotributylamine (PFTBA) prior to data acquisition. EPR spectra were recorded on a Bruker ESP 300 spectrometer interfaced to a computer with Bruker ESP1600 system software.

All chemicals, unless noted otherwise, were obtained from Aldrich and used as received.

Materials. Zeolites. Sodium-exchanged ZSM-5 (Si/Al = 20) was a Chemie Uetikon product obtained as a generous gift from Dr. V. Ramamurthy, Department of Chemistry, Tulane University, New Orleans, LA. The mean crystal lateral dimension of the silicalite was ca. 1 μm and that of ZSM-5 was ca. 0.3 μm as characterized by scanning electron microscopy. The external surface area of ZSM-5 was determined by the mercury porosimetry method[28] to be 16 m^2/g.

1,3-Diphenyl-2-propanone (DBK) (1) was purified by recrystallization from 5% (v/v) ether in hexane.

1-(2-Methylphenyl)-3-phenyl-2-propanone (o-MeDBK) (1-oMe) was synthesized following a method designed for 1-(4-methylphenyl)-3-phenyl-2-propanone using 2-(methylphenyl)-acetic acid instead of 4-(methylphenyl) acetic acid.[29] ^{1}H NMR: δ 7.35−7.26 (m, 3H), 7.21−7.11 (m, 5H), 7.11−7.02 (m, 1H), 3.74 (s, 2H), 3.71 (s, 2H), 2.13 (s, 3H). ^{13}C NMR: δ 205.9, 137.2, 134.2, 133.0, 130.6, 128.9, 127.6, 127.2, 126.4, 49.3, 47.5, 19.7. MS *m*/*z* (relative intensity): 224.05 (M$^+$, 2.6), 133 (4.0), 132 (6.6), 119 (2.1), 118 (4.2), 105 (100), 91 (69), 92 (24), 77 (15.8).

1,3-Di(phenyl-d_5)-2-propanone (DBK-d_{10}) (1-d_{10}) was synthesized as follows: Benzene-d_6 was treated with oxalyl chloride to yield benzoyl-d_5 chloride,[30] which was reduced with $LiAlH_4$ to yield benzyl-d_5 chloride.[31] The latter was treated with KCN and refluxed with a concentrated KOH solution.[32] The resulting acid was treated with thionyl chloride to yield phenyl-d_5 acetic chloride. Then the procedure of o-MeDBK synthesis was employed to produce DBK-d_{10}. ^{1}H NMR: δ 7.32 (s, 0.03H), 7.15 (s, 0.06H), 3.72 (s, 4H). ^{13}C NMR: δ 205.9, 133.9, 129.5, 129.2, 128.9, 128.7, 128.4, 128.0, 127.0, 126.7, 126.4, 49.1. MS *m*/*z* (rel int): 220.2 (M$^+$, 7.6), 123 (7.4), 96 (100).

1-[2-Methyl(phenyl-d_4)]-3-phenyl-2-propanone (o-MeDBK-d_4) (1-oMe-d_4) was synthesized as follows: To a 120 mL of $LiAlH_4$ solution in THF (1.0 M, 0.12 mol) was added 10 g of phthalic-d_4 acid (0.06 mol) to yield 8 g of (2-hydroxymethylphenyl-d_4)methanol (0.056 mol, 94% yield). The latter was stirred with 25 mL of hydrochloric acid (37 wt % aqueous solution) and extracted with ether. After drying over $MgSO_4$ the solvent was removed under vacuum and the product was purified by flash column chromatography to yield 6 g of (2-chloromethylphenyl-d_4)methanol (0.037 mol, 67% yield). The latter was treated with 40 mL of $LiAlH_4$ solution in THF (1.0 M, 0.04 mol) to yield 5 g of (2-methylphenyl-d_4)methanol (0.0396 mol, 107%). The latter was stirred with 20 mL of hydrochloric acid (37 wt % aqueous solution) to yield 4.1 g of (2-methylphenyl-d_4)methyl chloride (0.028 mol, 72% yield). Then the procedure for o-MeDBK synthesis was followed to yield the final product **1**-oMe-d_4. ^{1}H NMR (ppm): 7.35−7.25 (m, 3H), 7. 17−7.14 (m, 2H), 3.74 (s, 2H), 3.70 (s, 2H), 2.13 (s, 3H). ^{13}C NMR: δ 205.8, 137.0, 134.2, 132.9, 129.6, 128.8, 127.2, 49.2, 47.4, 19.6. MS *m*/*z* (rel int): 228.15 (M$^+$, 3.0), 137 (4.0), 136 (6.7), 119 (2.4), 118 (4.6), 110 (8.8), 109 (100), 108 (7.2), 92 (24), 91 (66), 82 (7.2).

1-(2-Methylphenyl)-3-(phenyl-d_5)-2-propanone (o-MeDBK-d_5) (1-oMe-d_5) was synthesized following the procedures of **1**-oMe-d_4 synthesis, using phthalic acid instead of phthalic-d_4 acid, and benzyl-2,3,4,5,6-d_5 chloride instead of benzyl chloride. ^{1}H NMR (ppm): 7.21−7.15 (m, 3H), 7. 11−7.05 (m, 2H), 3.73 (s, 2H), 3.71 (s, 2H), 2.12 (s, 3H). ^{13}C NMR: δ 205.8, 137.1, 134.0, 133.0, 130.6, 127.5, 126.3, 49.1, 47.4, 19.6. MS *m*/*z* (rel int): 229.15 (M$^+$, 1.8), 133 (3.9), 132 (5.8), 124 (1.7), 123 (4.3), 105 (100), 97 (22), 96 (76.8), 77 (16.7).

1,3-Bis(2-methylphenyl)-2-propanone (o,o′-diMeDBK) (1-o,o′DiMe) was synthesized following a published procedure for the synthesis of 1,3-bis(4-methylphenyl)-2-propanone using 2-(methylphenyl)acetic acid instead of 4-(methylphenyl)acetic acid.[29] The product was purified by column chromatography with hexane/ether (19:1 v/v) and was recrystallized from hexane/ether as white crystals. ^{1}H NMR: (ppm) δ 7.22−7.13 (3H, m), 7.09−7.06 (2H, m), 3.73 (4H, s), 2.17 (6H, s). ^{13}C NMR: (ppm) δ 205.9, 137.1, 133.1, 130.7, 130.6, 127.6, 126.4, 47.5, 19.8. MS *m*/*z* (rel int): 238.20 (M$^+$, 1.8), 132 (3.4), 133 (2.1), 105 (100), 77 (18).

2,4-Diphenylpentan-3-one (2) was synthesized with iodomethane and **1** following a published procedure[25] The meso:

(28) Abrams, L.; Keane, M.; Sonnichsen, G. C. *J. Catal.* **1989**, *115*, 410−419.

(29) Turro, N. J.; Weed, G. C. *J. Am. Chem. Soc.* **1983**, *105*, 1861−1868.

(30) Sokol, P. E. In *Organic Syntheses*; Baumgarten, H. E., Ed.; John Wiley: New York, 1973; Coll. Vol. 5, p 706.

(31) Nystrom, R. F.; Brown, W. G. *J. Am. Chem. Soc.* **1947**, *69*, 1197−1199.

(32) Ruhoff, J. R. In *Organic Syntheses*; Blatt, A. H., Ed.; John Wiley: New York, 1943; Coll. Vol. 2, p 292.

d,l ratio was determined by ^{1}H NMR to be 92:8 comparing the chemical shifts of the diastereomerically pure *meso*- and *d,l* -**2**. ^{1}H NMR (ppm): δ 7.37−6.95 (m, 10H) (consisting of 7.37−7.27 and 7.22−7.13, m, 6.24H and 7.01−6.95, m, 3.67H), 4.0−3.7 (m, 2H) (consisting of two quartets: 3.88, 1.81H, J = 7.04 Hz and 3.77, 0.16H, J = 6.88 Hz), 1.4−1.1 (m, 6H) (consisting of two doublets: 1.38, 5.68H, J = 7.04 Hz and 1.25, 0.48H, J = 6.87 Hz). ^{13}C NMR: δ 211.5, 210.5, 140.2, 128.6, 128.2, 127.0, 51.7, 18.5. MS *m*/*z* (rel int): 238.05 (M^+, 3.3), 133 (7.3), 105 (100), 77 (16).

2-(2-Methylphenyl)-4-phenylpentan-3-one (2-oMe) was synthesized by **1-oMe** with iodomethane following the same procedure as for **2**. ^{1}H NMR (ppm): δ 7.34−6.93 (m, 9H), 4.2−3.4 (m, 2H) (consisting of 4 quartets: 4.06, 0.56H, J = 6.97 Hz; 3.91, 0.35H, J = 6.82 Hz; 3.79, 0.55H, J = 7.07 Hz; 3.65, 0.37H, J = 6.86 Hz), 2.3−1.9 (m, 3H) (consisting of two singlets: 2.20, 0.88H; 2.06, 1.61H), 1.45−1.10 (m, 6H) (consisting of four doublets: 1.38, 1.98H, J = 7.10 Hz; 1.34, 1.69H, J = 7.01 Hz; 1.28, 1.11H, J = 6.90 Hz; 1.21, 0.92H, J = 6.82 Hz). ^{13}C NMR: δ 211.8, 211.2, 141.2, 140.4, 139.6, 138.5, 135.9, 135.8, 131.0, 130.6, 129.1, 128.4, 128.1, 128.0, 127.8, 127.2, 127.2, 127.0, 126.9, 126.9, 126.3, 51.4, 51.0, 48.0, 47.0, 19.6, 19.5, 19.0, 18.5, 17.9, 17.4. MS *m*/*z* (rel int): 252.10 (M^+, 1.7), 147 (5.0), 146 (4.3), 133 (1.4), 132 (1.4), 119 (100), 105 (52.5), 91 (16), 77 (16).

2,4-Di(phenyl-d_5)pentan-3-one (2-d_{10}) was synthesized by **1-d_{10}** and iodomethane following the same procedure as for **2**. ^{1}H NMR (ppm): δ 7.20−7.16 (m, 0.09H), 6.98 (s, 0.06H), 3.92−3.73 (m, 2H) (consisting of two overlapping quartets: 3.92−3.84, 1.82H, J = 7.04 Hz, 6.93 Hz and the third quartet: 3.77, 0.16H, J = 6.86 Hz), 1.39−1.24 (m, 6H) (consisting of two overlapping doublets: 1.39−1.35, 5.58H, J = 7.06 Hz, 6.85 Hz and the third doublet: 1.25, 0.49H, J = 6.88 Hz). ^{13}C NMR: δ 211.5, 210.5, 208.2, 140.9, 140.1, 134.3, 128.3, 128.0, 127.7, 127.4, 126.8, 126.4, 126.1, 51.6, 18.5. MS *m*/*z* (rel int): 248.25 (M^+, 1.6), 138 (4.8), 110 (100), 83 (11).

3,5-Diphenylheptan-4-one (3) was synthesized by **1** and iodoethane following the same procedure as for **2**. It was obtained as white crystals. ^{1}H NMR: δ 7.16−7.12 (m, 6H), 6.96−6.93 (m, 4H), 3.60 (t, 2H), 2.10−1.94 (m, 2H), 1.75−1.60 (m, 2H), 0.78 (t, 6H). ^{13}C NMR: δ 210.9, 138.7, 128.7, 128.5, 127.0, 60.7, 26.2, 12.4. MS *m*/*z* (rel int): 266.15 (M^+, 3.2), 147 (7.6), 119 (76), 91 (100).

6,8-Diphenyltridecan-7-one (4) was synthesized by **1** and 1-iodopentane following the same procedure as for **2**. It was obtained as an off-white liquid at room temperature. ^{1}H NMR: δ 7.40−7.10 (m, 6H), 6.96−6.93 (m, 4H), 3.68 (t, 2H, J = 7.41 Hz), 1.99−1.91 (m, 2H), 1.69−1.57 (m, 2H), 1.3−1.0 (m, 12H), 0.82 (t, 6H, J = 6.6 Hz,). ^{13}C NMR: δ 210.9, 139.0, 128.6, 128.5, 126.9, 58.8, 33.0, 31.8, 27.4, 22.6, 14.2. MS *m*/*z* (rel int): 350.25 (M^+, 1.3), 189 (2.5), 161 (53), 91 (100).

All of the purified ketones were above 97% pure by GC analysis after column chromatography and/or recrystallization. Typical impurities in the **2** series are the corresponding compounds from mono- and trialkylation.

Sample Preparation. ZSM-5 was activated in a furnace at 500 °C for 2 h and was cooled in a desiccator to room temperature before use.

A typical sample preparation was as follows. A specific loading was achieved by stirring a weighed amount of ketone in a solution of 0.8 mL of isooctane with 300 mg of zeolite for an hour. After evaporation of the solvent under argon flow, the samples were dried under vacuum.

GC analysis was employed to determine the photolysis products with 1-phenyldodecane as an internal standard.

Photolysis. Typical photolysis conditions employed 100 mg of dried zeolite samples in a quartz cell equipped with a sidearm for vacuum degassing. After pumping to 1×10^{-5} Torr, the samples were irradiated for 8 min with a 450 W mercury lamp equipped with a chromate filter solution. The resulting photolyzed sample was (within 2 min) placed into the ESR cavity for ESR measurement. For peroxy radical detection, the samples were open to the air briefly after photolysis and degassed to 10^{-4} Torr (ca. 3 min), and then the ESR spectra were acquired. For NO scavenging, the samples were immediately connected to the vacuum line after photolysis, degassed, and equilibrated with the NO gas (previously deaerated) at 2 Torr. The EPR spectra of the sample were taken, and then the sample was photolyzed for another 8 min and the EPR spectra were taken again for comparison.

Product Analysis. The products of photolysis of **2** were extracted from zeolite by stirring the zeolite with benzene (0.5 mL per 100 mg of zeolite) overnight. Then 4,4′-dimethylbenzophenone was added to the slurry as an internal standard. The supernatant was analyzed by GC and GC−MS analysis. The identity of products was determined by comparison to commercial samples of 2,3-diphenylethane, styrene, and ethylbenzene on GC and on GC−MS. The ratios of each compound were determined by the integral of corresponding peaks on the GC trace assuming the same detector response. The mass balance was calculated by combining the amount of the starting ketones and all the products from GC traces, with the starting ketones calibrated against the internal standard.

Spectral Simulations. Computer simulations of the EPR spectra were performed on the Simfonia program (Bruker), assuming partially hindered rotation of the radicals, which averages the anisotropies but allows a significant broadening of the hyperfine lines. The simulation of EPR spectra of B and α-MeB radicals was based on published proton−electron hyperfine coupling constants.[33] The deuterium−electron hyperfine coupling constants for the phenyl ring perdeuterated B and α-MeB radicals were assumed to be about one-fifth of its protic counterpart.

The simulations of EPR spectra of α-MeBNit were performed with the following parameters. For *g* factor, $g_{xx} = 2.008$, $g_{yy} = 2.006$, $g_{zz} = 2.002$ were assumed. For A_{ii}(N), $A_{xx} = 4$ G, $A_{yy} = 4$ G, and $A_{zz} = 35$ G were obtained from calculation. Coupling constants from spectral simulations were 18 and 27 G for the two α-H's and 0.5 G for the protons in α-Me groups. The line width was set to be 3.5 G.

For the simulation of the EPR spectrum of α-$MeBO_2$, two components in the ratio of 1:1 were independently computed and added to provide a good fit with the experimental spectrum. The simulation of one component involves $g_{xx} = 2.0015$, $g_{yy} = 2.009$, $g_{zz} = 2.0029$ as *g* factor, and a line width of 4.3G for adsorption along the *X* and *Y* axes and 8.5 G along the *Z* axis. The simulation of the second component involves $g_{xx} = 2.001$, $g_{yy} = 2.0084$, $g_{zz} = 2.023$ as *g* factor and a line width of 4.7 G for adsorption along the *X* and *Y* axes and 10.0 G along the *Z* axis.

The simulations of EPR spectra of BO_2 employed $g_{xx} = 2.0033$, $g_{yy} = 2.0087$, $g_{zz} = 2.029$ as *g* factor and a line width of 10.0 G for adsorption along *X* and *Y* axes and 12.0 G along the *Z* axis.

Acknowledgment. The authors at Columbia thank the National Science Foundation for its generous support of this research (Grant No. CHE 98-12676). The research was supported in part by the Department of Energy and the National Science Foundation by Grant No. CHE 98-10367 to the Environmental Molecular Sciences Institute (EMSI) at Columbia University. M.F.O. thanks the Italian Ministero dell'Universita e della Ricerca Scientifica (MURST) for financial support.

JO011047L

(33) Conradi, M. S.; Zeldes, H.; Livingston, R. *J. Phys. Chem.* **1979**, *83*, 633−639.